Safety in Mines Research Advisory Committee

Final Project Report

The Relationship between ERR and seismic energy release for different geotechnical areas.

Authors

Steve Spottiswoode, John Napier, Alexander Milev and Fernando Vieira.

Research agency : CSIR Mining Technology

Project number : GAP 612c

Date : 13th April 2000

1 Executive Summary

Since the early 1960's, reduction of the volume of elastic convergence through the use of regional stability pillars has been the principal means of controlling mining-induced seismicity. This control measure has been exercised through limiting the average Energy Release Rate (ERR) to some figure, typically 20 or 30 MJ/m^2. Mines have responded by leaving large areas of reef as regional stability pillars. It has been found that seismicity has indeed decreased, but damaging seismicity has still occurred on active faces and even on the stability pillars. A re-assessment of ERR has therefore been needed.

We report here on a re-analysis of previous work on the relationship between ERR and seismicity. Data from four mines spanning the Ventersdorp Contact, Carbon Leader and Vaal Reefs were analysed using the MINF suite of programs (e.g. Spottiswoode, 1999). For each area considered, seismicity was compared to energy release (ERR times area mined), with seismicity and energy cumulated over time. Results were not in contradiction with previous work, but help to refine and consolidate certain ideas.

Based on our analysis, we recommend the following for application of ERR to current mine layout design:

1. The choice of value of ERR to be used must be made at each mine on the basis of local experience with rockburst damage.

2. The mine's average ERR should be calculated from ERR determined at all active working places.

3. High values of ERR should not be excluded from the average.

4. When high values of ERR are encountered, the area should be mined using special, or remnant, precautions.

5. There are large variations in the amount of seismicity per elastic energy release in different areas. Within any single area, the rate of seismicity per energy release is almost constant, varying by less than the variations between areas.

6. A mine may wish to reduce ERR in areas of higher seismicity per energy release and increase ERR is areas of lower seismicity per energy release, as long as the nominated average ERR is not increased. ERR could be **decreased** by various means, such installing backfill, decreasing spans or increasing pillar sizes. In the extreme, faces could be stopped. ERR could be **increased** by, for example increasing spans or decreasing pillar sizes.

7. Mines should continue using their current values of moduli and stope width until suitable numerical models are available to account for inelastic effects on a mine-wide scale. In general, a Young's modulus of about 70 GPa is used at mines.

8. Calculation of ERR through multi-step mining is numerically very consistent and is independent of grid size and order of mining. This method is closely related to the concept of the volume of elastic convergence. We recommend that computer programs that report ERR use this method when ERR is used as an indicator of seismicity.

9. We recommend that mines establish the practice of digitising, in a form suitable for MINSIM-type and modelling, or continue it where it is being done. Current approaches using CAD are unsuitable. Quantitative comparison with seismicity should be done routinely to identify those areas with an anomalously high or low rate of seismicity.

10. Analysis of seismicity alone does not provide an accurate measure of rockburst hazard or risk. To supplement the previous recommendation, mines should maintain an on-going database of damaging rockbursts. Similarly, the evaluation of the effect of backfill requires a study of in-stope measurements.

Further research in this area will most likely improve correlations between observed and modelled seismicity. This will be the main thrust of the GAP722 project starting in April 2000. The final objective of this project will be to provide more accurate tools for mine design. In doing this, we expect to obtain further insights into what controls the amount and character of seismicity.

Table of contents

Table of figures

2 Introduction

Energy Release Rate (ERR) is the most commonly used mine layout design parameter for minimising seismicity in deep-level mining, especially in the less heavily faulted Carbon Leader and Ventersdorp Contact reef. Commonly, mines have decided on levels of ERR that should not be exceeded on these reefs. Typically, values of 30 MJ/m^2 or less have been suggested.

The concept of ERR as a mine layout design criterion derives from several sources.

1. Theoretical considerations as written in the landmark paper by Cook et al (1966). These have been extensively amplified by Salamon (e.g. 1984) and Napier (1991).

2. The early use of strike stabilising pillars at ERPM mine (van Antwerpen and Spengler, 1982).

In early analyses at ERPM it was found that the amount of seismicity was proportional to the volume of elastic convergence in studies (McGarr, 1976 and McGarr and Wiebols, 1977). It should be pointed out here that there is a close relationship between ERR and the volume of elastic convergence. This proportionality was further confirmed by Spottiswoode (1988) for Blyvooruitzicht mine. He also showed a linear relationship between ERR and the number of rockbursts per area mined. Figure 2.1, from Vieira (1997, after Heunis, 1970) shows a similar linear relationship between ERR and the number of rockbursts. In contrast, Spottiswoode (1988) and Milev and Spottiswoode (1997) found large deviations from this simple linear relationship.

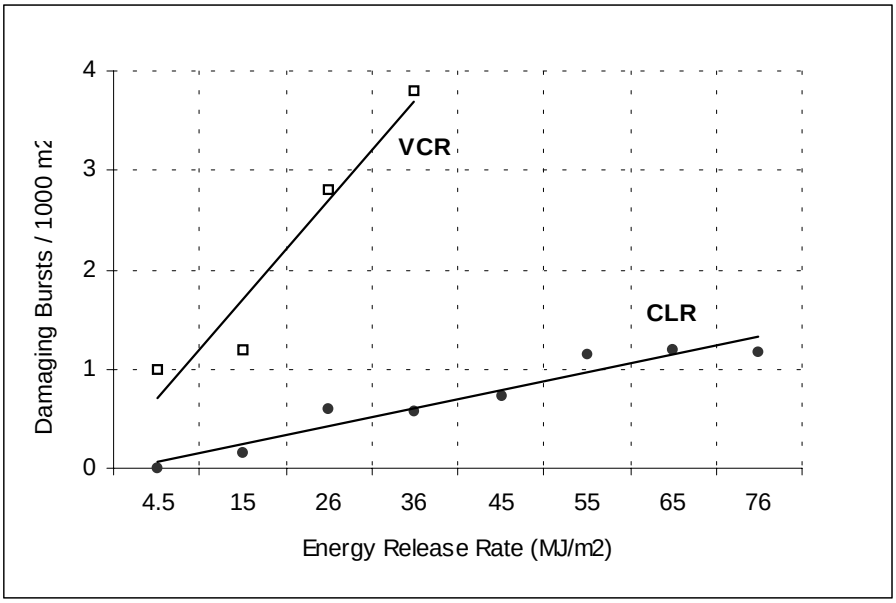

Figure 2.1 -The number of damaging bursts vs. ERR on the VCR and CLR for the period Jan. 1975 to Dec. 1976; from Viera (1997) after Heunis, (1980).

Why is there a deviation from a simple relationship between seismicity and ERR? Firstly, the linear relationship in Figure 2.1 was based on a large degree of averaging. Secondly, as shown by Milev and Spottiswoode (1997), a division of the host rock into different geotechnical areas has showed how differences can be associated with different geotechnical areas: hard and soft lava hanging-wall in their case. Thirdly, mining layouts at depth have generally become more complex over the last decades, with significant deformation and seismicity occurring on pillars and remnants (e.g. Ozbay et al, 1993).

Addressing all of these points calls for a more detailed mechanistic relationship between rock deformation and seismicity than is provided by ERR as modelled within an elastic rock mass. Spottiswoode (1997) took a small step towards this end by allowing for relaxation of on-reef stresses that exceeded a defined cap stress. He found that the ERR was better able to model the back-area seismicity in a region where strike-stabilising pillars were used when a cap stress of 250 MPa was applied

The effect of a small number of off-reef deformations on ERR was studied by Napier (1991). An important conclusion from this work was that off-reef energy release is in addition to on-reef energy release. This showed up a major problem with the approach of Spottiswoode (1997).

3 Theory

In any treatise of energy, it is useful to look at sources and sinks of energy. Gravitational potential energy is the source of the mechanical energy that must be distributed as mining takes place. This potential is released as the overlying rock move downwards and cause stopes convergence and an equal amount of downwards movement compressing the unmined regions.

The following are possible sinks of energy during mining:

1. Frictional energy (I in Figure 3.1 below)
2. Fracture energy (II below)
3. Kinetic energy (III below)
4. Strain energy in the removed material.
5. Strain energy in the remaining rock mass.

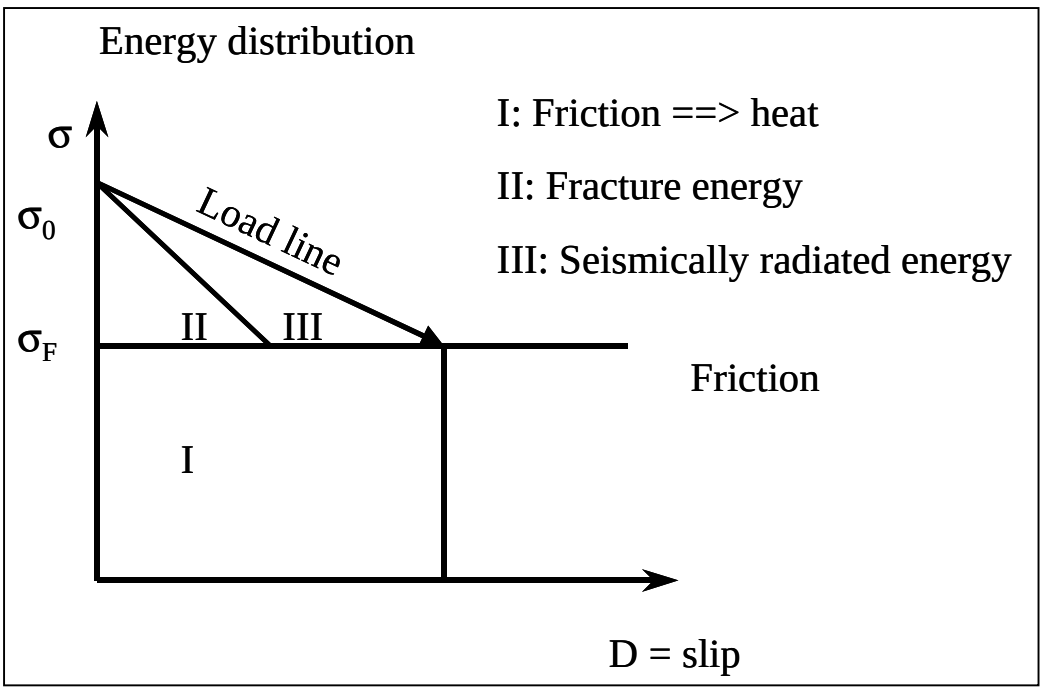

Figure 3.1 Partitioning of energy during shear slip (Jordan, 2000).

3.1 ERR in a perfectly elastic and homogeneous world.

The theory of ERR was introduced as a tool for mine layout design while making the assumption that mining takes place in perfectly elastic rock. When rock at the face is removed, generally by blasting, the remaining rock mass must find its new equilibrium. At the instant of removal of rock at the face, there is a stress imbalance. In the elastic world, this imbalance results in a dynamic relaxation and seismic waves are radiated. This energy per area mined is the ERR. The mathematics of this situation has been explored through many papers, principally by Salamon and co-workers (e.g. Salamon 1984).

The first practical application of ERR was the decision to leave strike stabilising pillars at ERPM mine (van Antwerpen and Spengler, 1982).

The use of ERR in mine design was formalised in the 1988 Industry Rockburst and Rockfall guide, see also Figure 1 above. Figure 1 shows a linear relationship between rockbursting per area mined and ERR. This was in good agreement with the recommendation by Cook et al (1966) that the volume of elastic convergence should be minimised to reduce the total amount of released energy. This figure shows remarkably good agreement between ERR and rock bursting. Spottiswoode (1988) also found a linear relationship between ERR and both seismicity and rockbursting, but found better agreement between seismicity and Volume Excess Shear Stress.

There are a number of problems with the concept of seismicity resulting directly from elastic ERR. For example

1. The rock around deep-level faces is intensely fractured and therefore the face is not as highly stressed as predicted by elastic theory.

2. Seismic events do not all occur at the moment of face advance.

3. The source mechanism of seismic events is predominantly shear either on geological faults or in previously solid rock. Classic elastic ERR relates to on-reef factors only and is therefore incompatible with the 3-D nature of shear zones that often extend many stope widths off-reef.

4. The energy associated with classic elastic ERR is released in approximately equal amounts during each day's face advance. The total energy, or moment, released by observed seismicity is dominated by the few largest seismic events that may occur months apart.

5. The largest events in the Carbon Leader and Ventersdorp Contact Reefs are associated either with regional stability pillars or with major geological features. In neither case does elastic ERR play a clear role.

Why were Heunis (1970) and Spottiswoode (1988) able to get good linear relationships between ERR and seismicity and rockbursts per area mined? We suggest two possible explanations:

1. Data from many areas were combined in ERR ranges, or bins. Without being too facetious, this could be called “super-averaging”. Quantification of the behaviour of any single area results in averaging of any variations within that area. Grouping areas together on the basis of similar values of ERR results in a further level of averaging. Hence we have “super averaging”.

2. At the time of the work of Heunis (1970), large variations in ERR were provided by increases in mining span and stabilising pillars were not yet being used at WDL. Spottiswoode (1988) considered ERR and also extended the Excess Shear Stress (ESS) concept to geologically less complex mining. He found distinct deviations from linear behaviour between seismicity and ERR for remnant mining. It is likely that the ERR model is less suited to complex mining situations.

Although ERR is derived from the compulsory energy released when mining, the relationship with seismicity is not as direct as predicted by the elastic theory. Anon (2000) and SIMRAC (1999b) go further and suggests that the real role of ERR in mine design is as an indicator of face stresses.

Given these problems, these is clearly a need to move beyond classic elastic ERR.

3.2 ERR when the face is crushed.

The dominant feature of rock conditions in deep-level stopes is the large number of face-parallel fractures in the hanging- and foot-wall. These fractures are nature’s way of relaxing the excessively high stresses that would have occurred near the face. In the elastic world, the stress ahead of the face of an infinite longwall is given by (SIMRAC, 1999a):

$$\sigma_Z = \frac{qx}{\sqrt{x^2 - l^2}} \qquad (1)$$

Where σ_Z = vertical stress

q = virgin stress

x = distance from mid-point of slit

l = half-span

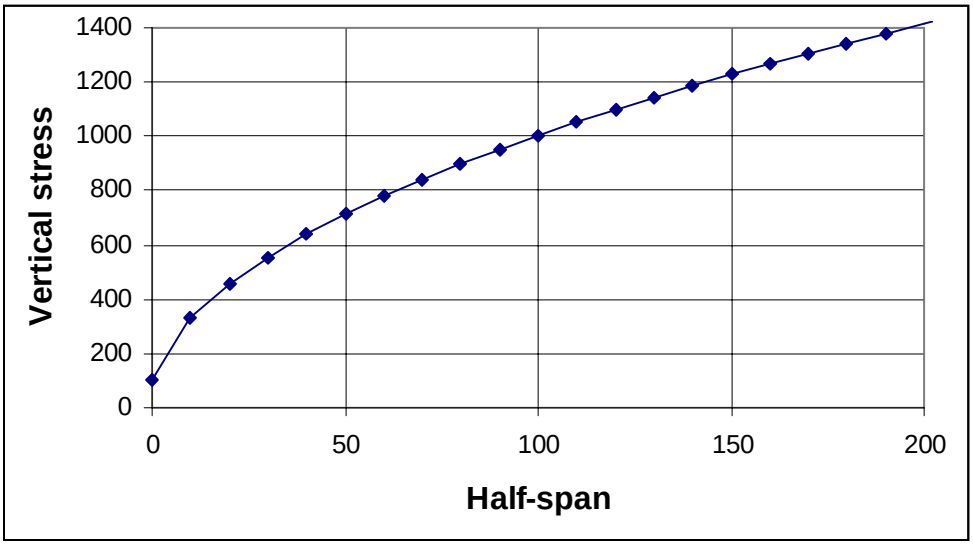

Figure 3.2 Stress at 0.5m ahead of the face of a slit for increasing span for virgin stress=100MPa.

Under deep level conditions, numerous fractures extend into the country rock around the advancing face. The depth of intense fracturing is typically several metres and illustrates most clearly the real-world departure from the elastic model. Furthermore, it is generally accepted that larger seismic events (M>≈2) involve shear slip extending 10's of metres from reef.

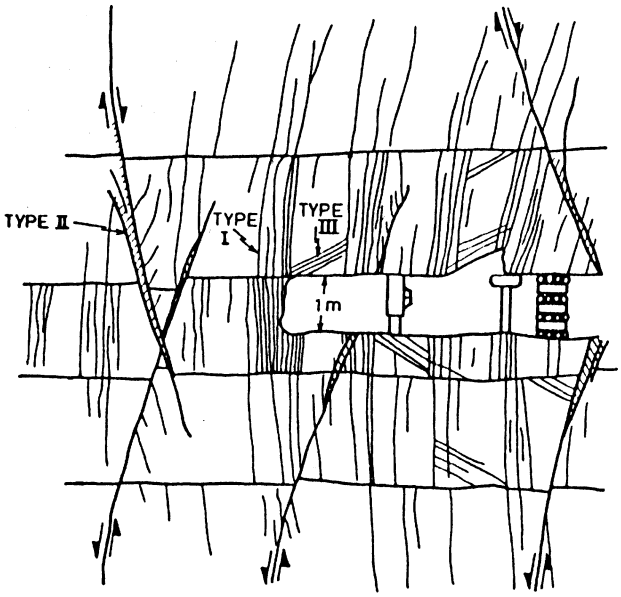

Figure 3.3 Typical arrangement of fractures around a stope face, from Malan (1999)

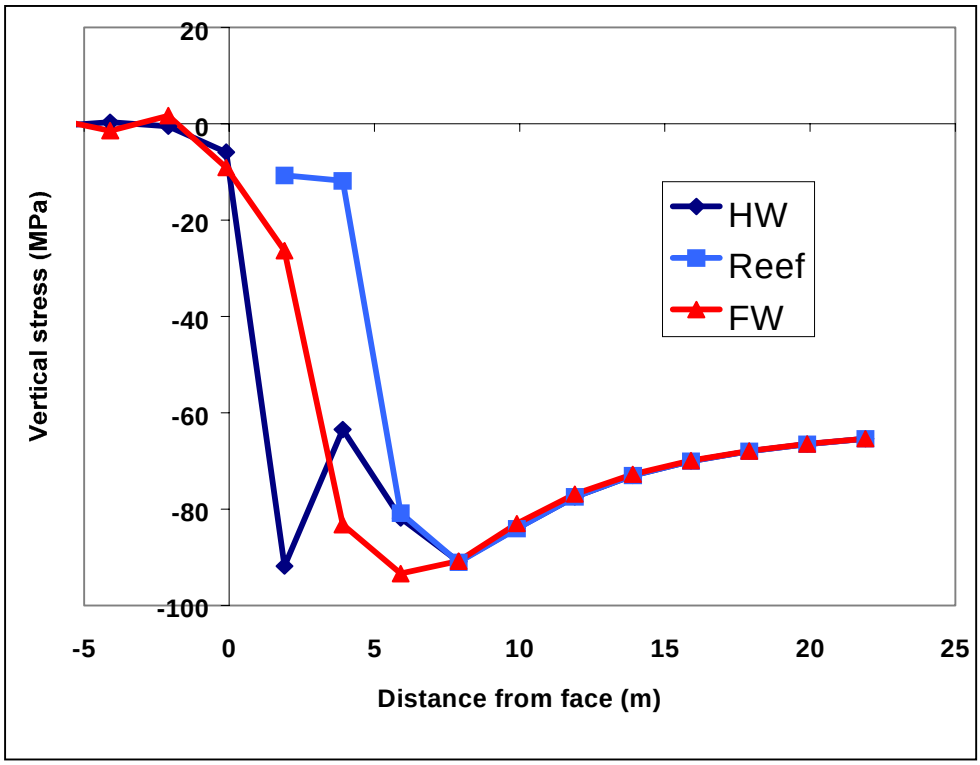

Figure 3.4 Modelled stress relaxation due to fracturing around a deep-level face (Sellers, 1997)

Sellers (1997) considered deformations and fracturing around a deep-level stope, using DIGS (Napier and Peirce, 1995). In Figure 3.4, we see that the on-reef stress ahead of the face can relax to about 10 MPa, much less than the elastic stresses of many 100's of MPa (Figure 3.2).

It is clear, therefore, that the strain energy in the rock that is actually removed when the face is advanced has been almost totally relaxed under normal conditions. In the rare cases when this has not happened, the face is prone to face bursting. Our discussion of ERR must therefore move to another stage, namely considering the effects of this fracture zone on ERR.

3.3 ERR and a finite fracture zone.

The fracture zone around deep-level stopes is a manifestation of energy release and therefore may affect the ERR. We consider three important effects of this fracture zone on ERR.

1. The effective span is increased. This increases convergence and the ERR. The increased convergence has been has been modelled by Sellers (1997), who found an effective increase in span of several metres. An increase in effective span of several metres over a span of, say, 100 m is of little importance.

2. The fracture zone bulks when stress relaxed as the face passes by. This is a poorly understood process, but it could provide a very important mechanism for the high stresses seen in backfill (Gürtunca and Adams, 1991). It is difficult to measure the relative contributions of this and the previous effect. We will show that the energy changes associated with localised inelastic effects are small at the spans commonly encountered in deep-level mines.

3. The load on remnants, pillars and abutments is reduced. This results in a widespread increase in convergence, with increased ERR for mining over a wide area. This stress relaxation probably explains the common observation of less seismicity than might be expected for the very high values of ERR commonly encountered during remnant mining (e.g. Spottiswoode, 1988). The practical effects of ERR on abutments is considered in Section 5 below.

Much of the study of rock mechanics in deep-level mines is involved in understanding the development and later potential instability of the fracture zone. It is a major topic of the on-going SIMRAC GAP601 project. It is therefore beyond the scope of this report to provide any detailed analysis of the effect of the fracture zone. However, as the fracture zone gets left behind, the strain energy stored in it is different from the strain energy that would have existed in the elastic situation. In this section, we will consider the maximum effect that a fracture zone of finite extent might have on ERR.

The elastic solution of a perfect slit predicts a horizontal stress of (k-1)*σ_V on a stope hanging- or foot-wall. Tensile stresses cannot exist in a heavily fracture environment. We use the "missing" tensile stress as an indicator of the stress deviations from perfect elastic behaviour.

Let us consider a fracture zone with a height of "h" and an associated stress hydrostatic perturbation of 0.5 *σ_V. From elastic theory, the strain energy per area mined that is associated with this stress perturbation *(ERR_F)* is given by:

$$ERR_F = \frac{3(1-2\nu)h\sigma_V^2}{4E} \tag{2}$$

The elastic ERR (labelled here as ERR_E) for a slit of half-span "l" is (SIMRAC 1999):

$$ERR_E = \frac{\pi(1-\nu^2)l\sigma_V^2}{E} \tag{3}$$

The relative error (P) in ERR calculation is then:

$$P = \frac{f.h}{l} \tag{4}$$

Where we have f = 0.15 from equations (2) and (3). As typical stopes have half-spans in excess of 50 m and for fracture zone vertical extents of 10 m (Figure 3.3), we find that P = 0.03 << 1. In other words, the effects of the stress changes in the normal fracture zone on ERR is very small. Individual seismic events that involve shear slip >> 10 m in extent are obvious exceptions to this "normal" representation of fracturing around underground stopes.

As the increase in effective span is also of little importance, the major errors in ERR will be encountered for mining with remnants and pillars. This is a great pity because it is under these conditions that the greatest care should be taken in mine layout design.

3.4 ERR and seismicity

Figure 3.1 indicates that there is some causal link between ERR and seismicity. The proportion of released energy that is radiated as seismicity is dependent on many factors that are beyond the scope of the current report. Suffice it to say that work is currently underway in SIMRAC projects GAP 601 and GAP 603. This issue was also partially addressed by Spottiswoode (1999) and will be studied further under GAP 722 during the years 2000 and 2001.

4 Choice of moduli and stoping width

From the time that it was shown that the rock mass around deep-level stopes behaves in an elastic manner, the moduli used from modelling have been based on values measured in the laboratory. Typically values measured for Witwatersrand quartzites are: Young's modulus E=70 GPa and Poisson's ration $\nu = 0.2$. Estimates of in-situ moduli can be made from back analyses of measured deformation data and from seismic wave velocities.

Gürtunca and Adams (1991) studied stress and convergence in backfilled stopes and suggested that softer rocks and jointing combine to downgrade the rock stiffness to an effective $E \approx 40$ GPa. They concluded "The use of an in situ modulus is suggested as an interim solution until a new computer model which considers the joints, different layers and inelastic closures becomes available". This suggestion has not been universally accepted. One reason was that the use of a reduced modulus gives increased values of ERR and the whole concept of using the ERR as a design criterion is then difficult to apply universally. Also, the raw data that was used by in previous studies are not available.

Seismic wave velocities as used by mine-wide seismic networks are approximately 5 700 m/s for P waves and 3 700 m/s for S waves. For a rock density of 2700 KG/m^3, the dynamic moduli are E = 84 MPa and $\nu = 0.14$.

The papers presented at the SARES99 symposium in Johannesburg in September 1999 were scanned as an indication of values of Young's Modulus and Poisson that are commonly used in numerical modelling. A summary is presented in Table 1. Unless

otherwise stated, the applications were for the deep-level Witwatersrand gold mines. Further details on the named programs are obtainable in the papers themselves. The program names are listed here to provide some indication of the thrust of each study.

Reef or rock type	E, GPa	ν	Program used	Purpose	Reference
Vaal	-	-	MINSIM-W	ESS	Bosman
Vaal	50 & 70 (B)	0.2	MINSIM-W & MAP3D	ESS	Dunn and Laas
Merensky (platinum)	120 (L, E)	0.16	MINSIM-W & FLAC	Small pillars	Spencer and York
LG6 (chromium)	-	-	MINSIM-W & FLAC	Small, shallow pillars	Spencer
Merensky	-	-	MAP3D, FLAC & UDEC	Small, shallow pillars	York et al
Stillwater Mine	122 (U, E) & 55 (U, E)	0.3	"HICell" & UTAH3	Inelastic zones	Johnson et al
Vaal	40 (E) & 50 (E)	0.2	FLAC	Running dyke	Oelofse & Judeel
Quartzite	-	-	DIGS & FLAC	Extension fractures	Kuijpers
Generic	-	-	?	Extension fracture	Stacey & Wesseloo
Generic	70 (V, E)	0.2	MINF	Seismicity modelling	Spottiswoode
VCR	50 (B, E)	0.2	BESOL MS 3D & FLAC3D	Shaft design	Rangsamy et al
Carbon Leader	(E)	-	MAP3D	Seismicity modelling	Lachenicht & van Aswegen
Generic quartzite	70 (L, E)	0.2	ELFEN	Fracture & support	Roberts et al
Quartzite	80 (S)	0.2	WAVE	Dynamics	Hildyard & Milev
Typical Canadian	50 (L?, E)	0.3	SATURN (FE)	Joints	Simon et al
Typical Canadian	78 (E)	0.15	FE	Burst potential	Tang et al
VCR	-	-	MINSIM & MINF	Seismics & stress	Vieira
Merensky	63 (L) & 57 (L, E)	0.11	MINSIM & ELFEN	FOG	Watson & Roberts
VCR & Elsburg	50	-		Shaft stability	Singh & MacDonald

Table 1. List of moduli used in papers presented at SARES99. E = Young's modulus and ν = Poisson's ratio.

At least 13 different computer programs were used in the 19 papers in Table 1.

Code	Explanation
B	Back-analysis from underground measurements
L	Laboratory testing
E	Explicit inelastic deformations applied
U	Determined from in-situ measurements underground
S	Estimated from seismic wave velocities measured underground
V	Not in text, but presented verbally.

Table 2. Codes for summarising motivation for use of moduli.

It is clear from the summary of the SARES99 papers that there is no universally accepted way of selecting moduli. In most of the small-scale studies, laboratory values (E≈70 GPa) were used and inelastic effects were explicitly modelled. In mine-wide studies, some papers used "typical" laboratory values, while others used lower values based on back-analyses of deformations measured underground.

Allowance for inelastic rock deformation increases the convergence (Spottiswoode 1999) in a manner similar to that achieved by reducing the modulus (Gürtunca and Adams, 1991). These models should be allowed to mature (e.g. GAP722, 2000/2002) and should carefully calibrated against underground measurements. The major concern of Gürtunca and Adams (1991) was related to problems with understanding the effect of backfill on stopes within an elastic environment. These problems can only be addressed through comparisons of observed with modelled convergences and/or stresses.

In summary, the negative implications that reducing the modulus have on ERR are greater than the short-term benefits of applying reduced modulus. The same applies to altering the stope width to achieve the same effect.

5 Calculation methods

ERR is the spatial rate of energy release, or work done in relaxing the stress at the face to zero. ERR is calculated in either of two ways, face ERR or multi-step ERR.

5.1 Face ERR

Face ERR is defined as one half of the product of stress ahead of the face (σ_F) and the convergence behind the face (C_F), where σ_F and C_F are taken at the mid points of elements immediately on either side of the face, see equation (5). This definition is easy

to conceive, but difficult to apply in numerical codes unless the face is grid-parallel. Special corrections are necessary for the more general case of irregular face outlines.

$$ERR = 0.5\ \sigma_F\ C_F \quad (5)$$

This method of calculating ERR has a number of merits. It can be calculated from the solution of a single mining layout; no actual mining is required. Furthermore, as applied in MINSIM (Napier and Stephansen, 1987), it can be calculated using the convergence values only, although this requires careful manipulation of values when the face is not fully grid-aligned.

1. It describes the ERR at that instant in time.
2. It is a measure of the face stress (SIMRAC 1999b).
3. Face ERR is very dependent on the assumption of an elastic rock mass.

5.2 Multi-step ERR

Multi-step ERR defines ERR in terms of the stress before mining and the convergence after mining. In this sense, it becomes equal to the work done in mining each element. The basic definition of work done by a constant force (F) acting over a distance (D):

$$W = F.D \quad (6)$$

In general, force may vary and equation (2) should be written as

$$W = \int F dD \quad (7)$$

From linear elasticity, deformations follow straight load lines and this equation can be written as:

$$W = (F_2 + F_1) * (D_2 - D_1) / 2. \quad (8)$$

This equation must be applied to all components of force. In the case of cracks, both normal and shear must be considered.

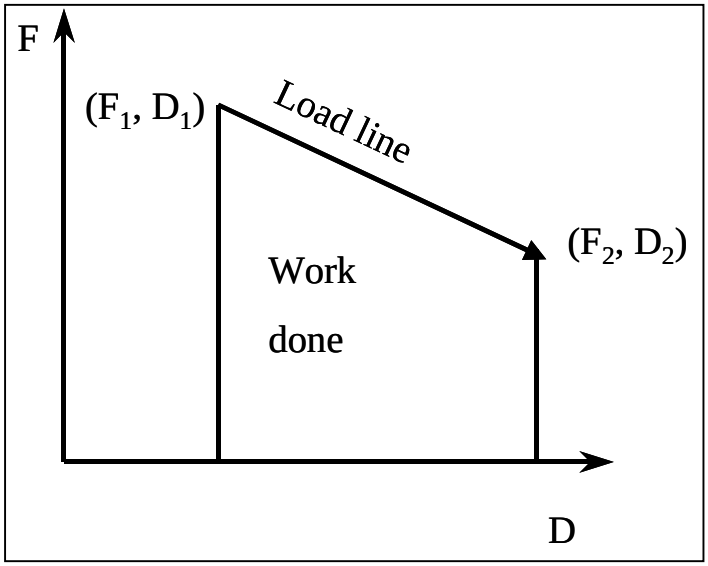

Figure 5.1. Sketch of work done by a force over a distance.

5.2.1 Testing Multi-step ERR

Multi-step mining simulation should aim at following the history of deformation, stress and energy release on each element as mining progresses. In the ultimate situation, each actual face advance is considered and seismicity is generated. As the rock deforms in a time-dependent manner (Malan, 1999), time steps between blasts are also needed for complete modelling. In such modelling, the amount of seismicity is controlled by the area mined and the degree of instantaneous stress drop during each slip event. However, for this report we are only addressing the issue of ERR.

At this stage we point out that all the simulations used in this report were performed using the program MINF, developed by Spottiswoode (1997, 1999 and many recent extensions). The program MINFOUT was used for certain post-processing. The recently developed MINSIM 3D viewer, developed in-house at CSIR Miningtek, was used for displaying data graphically. We used Young's modulus E=70 GPa and Poisson's ration ν = 0.2 for all MINF runs.

In Figure 5.2 we show the results of one of many calibration exercises to validate the MINF code. The mine layout consisted of an infinite longwall, aligned either grid-parallel or at 45^0 to the grid. There are two sources of error in the modelling.

1. The standard "quarter-grid" effect (Ryder and Napier, 1985) provides a small error in the modelled span. This error exaggerates the ERR somewhat and is therefore in the same sense as the effect of inelastic deformations. No attempt is therefore made to apply corrections at this stage.

2. A further increase in ERR at larger spans results from MINF considering the mining as an infinitely repeating pattern. This is clearly a disadvantage when modelling deformation around isolated mining. In many practical underground mining conditions, however, the world outside of the modelled area is mined in a manner similar to that inside the modelled area and this error is also neglected. When using MINF care should be taken to treat modelled deformations around the edges of the modelled area with caution. Of course, the same rule also applies when using MINSIM if there is mining nearby that is not included in the model.

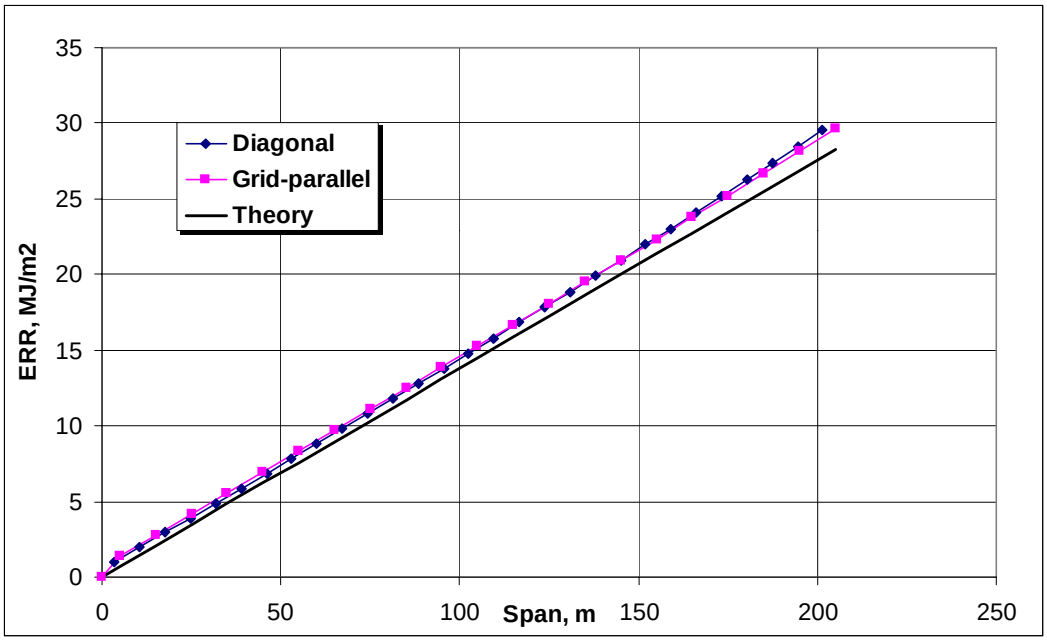

Figure 5.2 Comparison between theoretical and modelled ERR for an infinite longwall, aligned grid-parallel or at 45^0 to the grid pattern.

Next we simulate mining of a square block of ground, 160 m on a side, using multi-step mining. The solution program MINF and reporting program MINFOUT were used to do the simulations and reporting that is presented here.

Figure 5.3 show mining of this ground in three different ways. If the ground is viewed in the conventional sense of strike running from left to right and with some dip from top to bottom, the mining sequence can be described as follows.

A. A single longwall mining along strike.

B. Two shorter longwalls. The upper longwall mined first, followed by the lower longwall.

C. Mining from the outside inwards. The old adage of "mine towards the solid" is still considered best practice in the mining industry, in South Africa and elsewhere. Method "C" is therefore considered to be the worst way of mining this ground as severe rockbursts are expected during the later stages of mining.

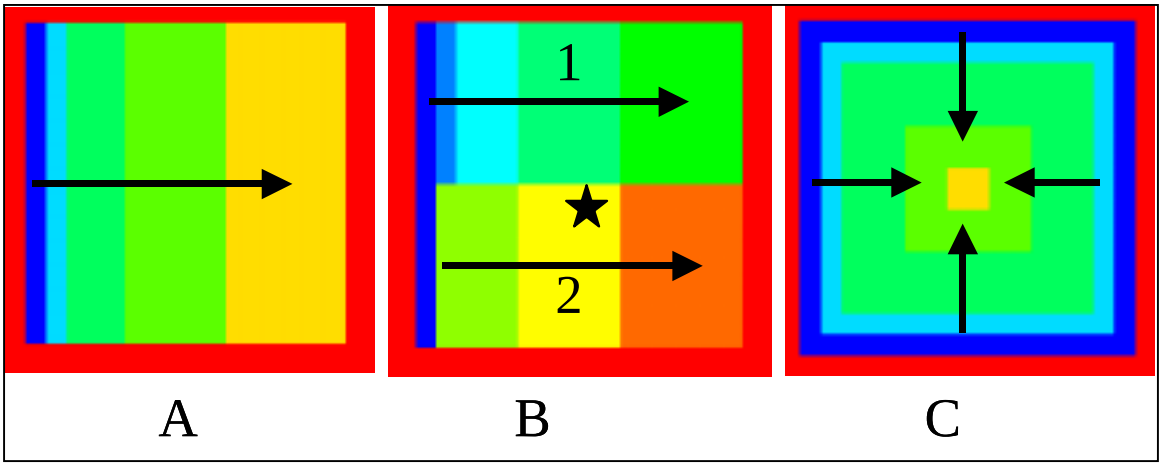

Figure 5.3. Sequences of extraction of a square block of ground as indicated by shading and arrows. The star marked "B" is the benchmark position used in Figure 5.5.

Figure 5.4 shows how the released energy cumulates during mining of the entire area. We can see that the same amount of total energy is released in all three cases. Each shaded area in the figure represents a mining step, with the arrows indicating the direction and order of mining. The ERR during each mining step and for each situation is given by

the slope of its curve. As expected, mining method C shows the highest ERR at the last stage of mining.

If there is indeed a linear relationship between ERR and seismicity per area mined, then the total amount of seismicity would be the same for all mining methods for mining any area. This is most clearly expressed as the basic motivation behind the recommendation from Cook et al (1966) to mine in such a way as to reduce the total volume of convergence. According to this, the total amount of seismicity depends only on the final mine layout.

Currently, mines usually attempt to reduce variations in ERR and to mine close to some average value. This is not always possible. All the curves in Figure 5.4 show increasing ERR, although mining method C shows the most extreme values towards the end.

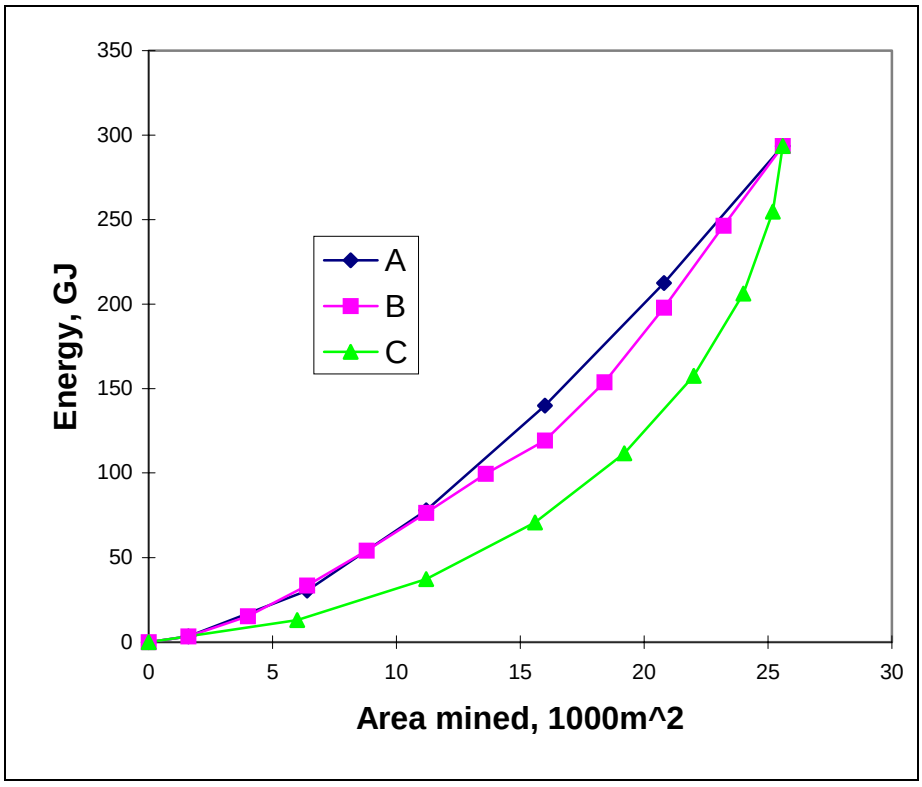

Figure 5.4 Cumulative energy release as a function of cumulative area mined.

The total amount of energy was the same whether the area was mined in small or large steps. The mining steps for options A and B advance in bands of up to three elements at

a time. The program MINF also allows for interpolation of these steps into small steps of single elements at a time. In all cases, the cumulative energy release amounts to the same total, within a tiny numerical round-off error. When each square element was subdivided into 4, 16 or 64 smaller elements, the total energy release decreased slightly, in accordance with the quarter-grid error (Ryder and Napier, 1985).

Spottiswoode (1997) analysed seismicity using a limit, or cap, stress at each element. Let us briefly consider the effect of this stress limit on ERR. Comparison with seismic data by applying a cap stress is not be considered in this report.

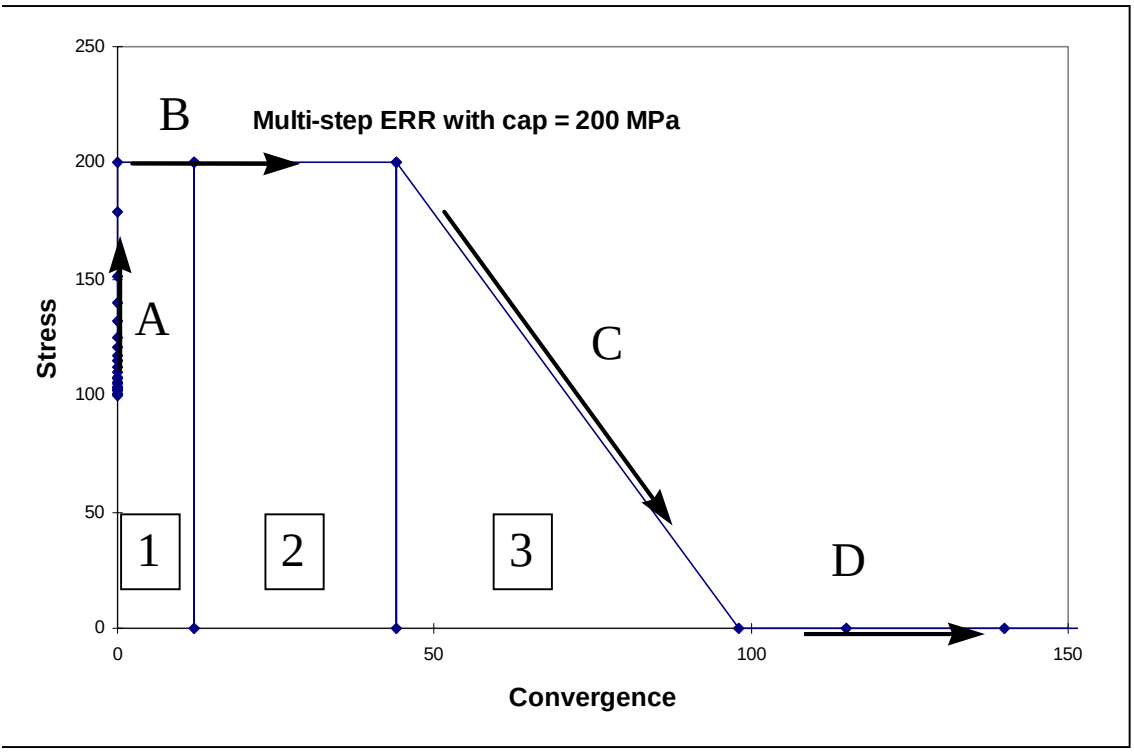

Figure 5.5. Energy release on a typical element when a cap stress of 200 MPa is applied. An element at the top of the lagging longwall in Figure 5.3B was chosen.

Each element can go through up to five stages in this stress-convergence plot.

A. Increase from virgin stress up to the cap stress.

B. Convergence as the element crushes to keep the stress from exceeding the cap stress. In this case, this stage this took place over two mining steps, labelled 1 and 2 here.

C. A stress release along the load line down to zero stress at mining step labelled 3 here.

D. Further convergence at zero stress.

E. (Not shown) Increase in stress when the stope is totally closed or backfilled. When backfilled, the stress increase follows the stress-deformation curve of the backfill.

5.2.2 Meaning of high ERR areas.

We see in Figures 5.3 and 5.4 above that it is difficult to mine to a constant level of ERR. This situation currently only occurs on mature longwalls between strike stabilizing pillars. As mining progresses in a typical mine, the deeper levels are accessed at a later stage than the shallower levels, as typified in Figure 5.6. Here the lower longwall lags the upper longwall by 160 m. In Figure 5.7, we see that the ERR on the actively mined face elements, assuming elastic behaviour, reaches almost 80 MJ/m^2. Modelling using a grid size smaller than 5 m would increase this maximum further. One may sympathise with the view at some mines that these extreme values be rejected when calculating the average ERR.

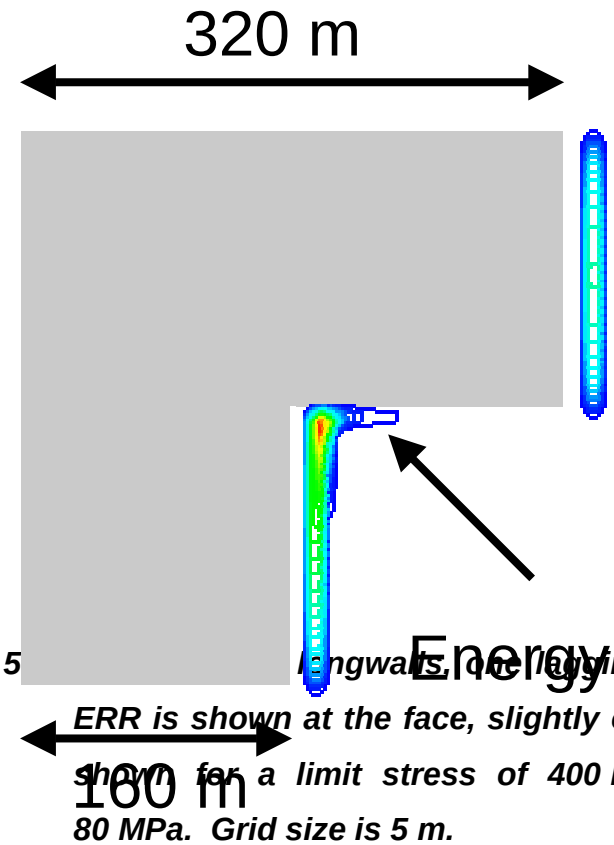

Figure 5 longwalls, one lagging the other. The multi-step ERR is shown at the face, slightly offset for clarity. The ERR is shown for a limit stress of 400 MPa and a virgin stress of 80 MPa. Grid size is 5 m.

Rockbursts under these conditions have not been found to be many times worse than normal. The common explanation is that the rock at the face has already been stress relaxed during growth of the south abutment of the upper longwall. Where the highest level of ERR is expected, normal or even easier conditions are encountered away from the immediate effect of the face-parallel fractures. We will try to show that it is **not** correct to reject these high values out of hand.

We modelled the situation in Figure 5.6 with a cap stress of 400 MPa (Spottiswoode, 1997 and Figure 5.5). In Figure 5.7, we show the energy released at face elements that are advanced.

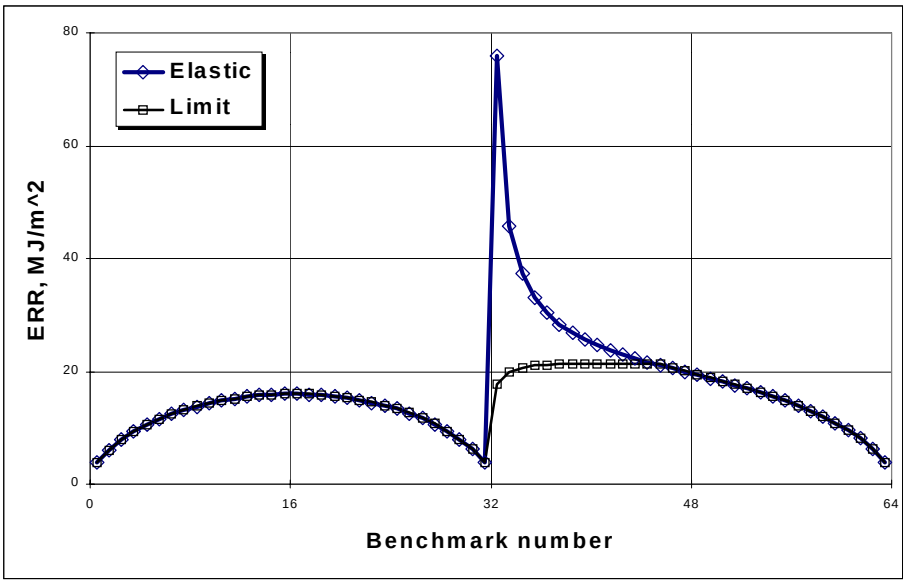

Figure 5.7 Total energy released by mining one element at the face in the mining geometry of Figure 5.6. The ERR is based on modelling with infinite strength (elastic) and with a limit stress of 400 MPa. Mining took place in a virgin stress of 80 MPa. The upper longwall is represented by benchmarks 1 to 32, while the lower longwall continues from 33 to 64. Benchmark numbers 33 to 64 are listed in column one and rows 33 to 64 in Table 3.

The effect of this cap stress on the ERR in the "anomalous" area was dramatic, with the maximum value of ERR decreasing from 76 MJ/m^2 to 21 MJ/m^2. The reduced ERR extended some 60 m along the face. This raises some important questions that we will attempt to address.

1. What happened to this energy?

   In determining the ERR only the energy released at the face was considered for Figure 5.7. As can be seen in Figure 5.6 and Table 3, energy is released along the South abutment and ahead of the face on the upper part of the lower longwall. The total energy released using the cap model was only about 2% greater than that released using the linear elastic model. If there were pillars involved, this increase could have been substantially more (Spottiswoode, 1997).

2. Why does the ERR have a constant value at about 21 MJ/m^2 for much of the lower longwall?

   The stress on these elements had already been limited to the cap stress of 400 MPa during the previous mining step. Convergence, and accompanying energy release, had already taken place on these elements in one or more previous mining steps in a manner similar to the regions 1 and 2 in Figure 5.5. The ERR on the face in Figure 5.7, and column #1 in table 3, was calculated from the energy released as shown diagrammatically in region 3 in Figure 5.5.

   The energy release when an element is mined is controlled by the local stiffness, or the ability of other elements to accept it load. The local stiffness along a straight face is the same. The same initial stress of 400 MPa then leads to the same value of ERR on the face.

3. Why does the ERR decrease towards to top of the lower longwall?

   This is a somewhat counter-intuitive result, as one might expect this corner to be "softer" due to the 270^0 expanse of mined out area around it. However, in the elastic model this corner was found to be **stiffer** than the longwall as a whole, having a value of 126 GN/m. The stiffness decreases rapidly to about 93 GN/m before increasing again to 117 GN/m at the bottom of the longwall. It must be noted that the stiffness, as applied here, is a function of grid size. As the energy release is inversely proportional to the stiffness for a fixed stress change, we see a decrease in ERR at the corner where the bottom longwall meets the abutment.

Row #	Energy release, MJ.	On columns in front of the face				
33	444	494	243	136	87	63
34	498	554	216	17		
35	516	530	16			
36	524	369				
37	529	276				
38	531	213				
39	533	168				
40	534	132				
41	535	104				
42	535	80				
43	536	59				
44	535	41				
45	535	24				
46	533	10				
47	517					
48	502					
49	486					
50	472					
51	456					
52	441					
53	424					
54	407					
55	389					
56	370					
57	348					
58	325					
59	300					
60	271					
61	239					
62	201					
63	156					
64	96					

Table 3 Energy release values, in MJ on the lower longwall. The first column represents the energy release as the face was advanced by one element. Each of these elements must be divided by 25 m^2 to obtain the ERR. The top row represents the energy released through yield on abutment.

6 Data analysis

Data from four mines have been analysed to test for the role of ERR on seismicity. Mining areas were digitised and gridded during previous projects. Seismic data were made available by the mines concerned. We only used data sets that were available in suitable format, namely some that were prepared as part of three previous, much larger, projects.

Large-scale, multi-step digitising suitable for MINSIM-type modelling is not currently available from the mines.

In most of the previous studies relating seismicity to ERR (e.g. McGarr and Wiebols, 1977 and Heunis, 1980, Figure 2.1), the amount of seismicity or rockbursting per area mined was compared to ERR. In this report we show one of these graphs, but have mostly aimed the work at looking at the progressive cumulative seismicity as a function of the cumulative energy release. The objective of these graphs is to highlight differences and similarity of the behaviour of areas over time. The total energy released (E) was simply:

$$E = W^2 * \Sigma \, ERR \qquad (9)$$

Where W = grid size and the summation was taken over all elements that were mined in each area and in each time period. As no cap stress is applied in this analysis, the energy is only released on elements that are mined in each step.

Cumulative observed seismicity was initially expressed in terms of ΣM_0, the cumulative seismic moment. It will be seen (e.g. Figures 6.2 and 6.5) that ΣM_0 was often dominated by large jumps caused by the largest events in the area. This is a common phenomenon as the largest few events account for most of the total seismic moment and seismic energy within any area.

To obtain a smoother relationship between cumulative seismicity and cumulative energy, we downgraded the effect of the largest events by using ΣN_F, where

$$N_F = 10^{M-4.25} \qquad (10)$$

When a region or time period is considered for comparing seismicity with modelling, difficult decisions must be made whether to include or exclude particular large seismic events. The largest events can dominate the total seismic moment or energy within any subset of seismic data. It will be shown in section 7 on error analysis that estimates of ΣN_F are less prone than ΣM_0 to error. Furthermore, Milev and Spottiswoode (1997) showed that N_F was more descriptive of damage than M_0. The largest events were found to be less damaging per unit of seismic moment than the smaller events. The plots using ΣN_F are therefore not only smoother than the plots using ΣM_0 but also more relevant as a means of characterising the behaviour of any area in terms of rockburst damage.

Simulating rock deformations around an entire mine in any level of detail is only possible by compromising the resolution, or element size. To reduce this effect, each mine was divided into regions for the purposes of modelling. Inside these regions, sub-regions (also

called seismogenic regions or simply polygons) were identified. Seismicity in terms of ΣM_0 and ΣN_F was then compared to the cumulative released energy within these sub-regions.

The digitised mine outlines were used to prepare a pattern using the MINSIM pre-processor program. Patterns were created to describe the history of mining of the reef on a coarse scale of 64 by 64 elements. The MINF code used the percentage-mined description on each element to obtain better resolution when each element was enlarged to form 16 (4 by 4) elements, bring the “problem” size up to 256 by 256 elements. Each element was then approximately 10 m on a side, allowing us to simulate pillars with reasonable accuracy across areas of 2.5 km by 2.5 km. As before, we used Young’s modulus E=70 GPa and Poisson’s ration ν = 0.2 for all runs.

Once sub-regions are identified within any modelled region, the code MINFOUT was used to generate a table containing summary information for the region itself and each sub-region. Data from this table was used to generate the plots summarising the relationship between seismicity and mining, using the EXCEL spreadsheet program from Microsoft Corporation. The earliest date was used as a base and only changes from this date were considered.

The following analyses were not undertaken using the limit, or cap stress. This will be done early in the forthcoming project GAP 722 and it is hoped that better correlations between seismicity and mining will be found.

6.1 Ventersdorp Contact Reef (VCR)

The VCR data sets used in this study was previously accumulated under SIMRAC project GAP 102 (Roberts et al., 1997).

6.1.1 Kloof Gold Mine

The VCR in Kloof Gold Mine is classified into several different geotechnical regions; "hard"' (Alberton) lava hangingwall with quartzite-conglomerate footwall and "soft"' (Westonaria) lava hangingwall with quartzite-conglomerate footwall occur most widely.

The seismic data set consisting of 32 438 seismic events recorded by the Gold Fields Seismic System over the period 1983 to 1995 were analysed using eight dates, spanning seven time periods. The recorded events range in magnitude from -2.0 to 4.9. The

southwest part of the mine (KLF1) showed a higher level of seismic activity than the northeast part. The distribution of the strong seismic events (M • 2.0) is shown in Figure 6.1.

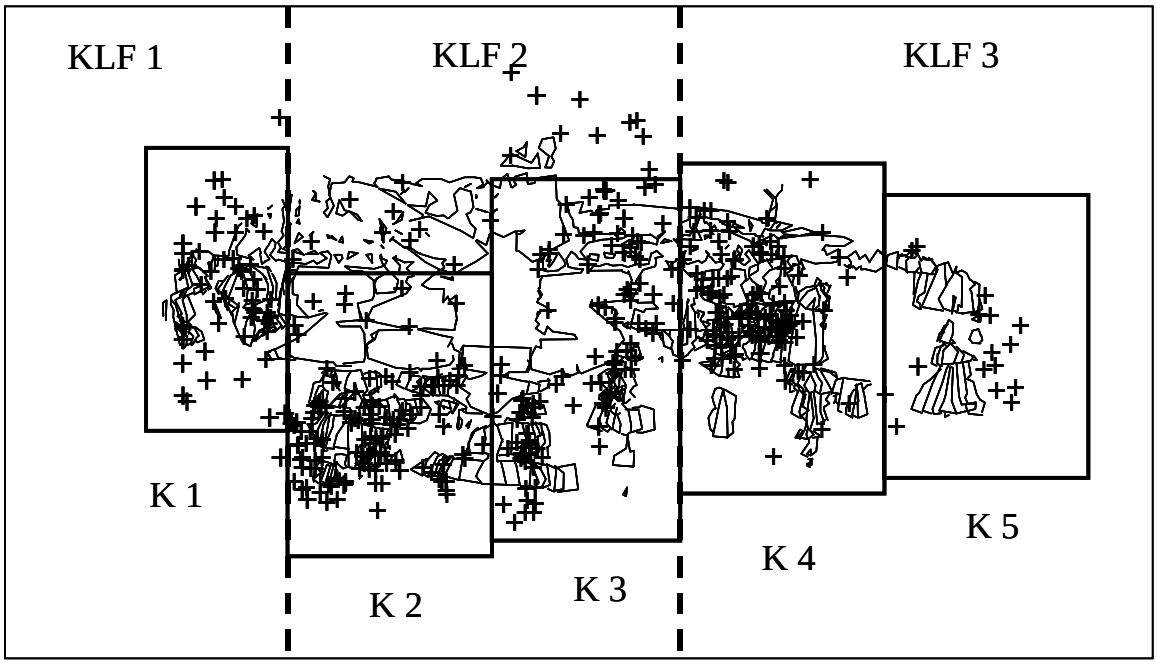

Figure 6.1 Kloof Mine: Mine plan with location of seismic events with magnitude M • 2.0.

Three regions (KLF1, KLF2 and KLF3) were used for the MINF solution. Five sub-regions (K1 to K5) were identified within the three regions.

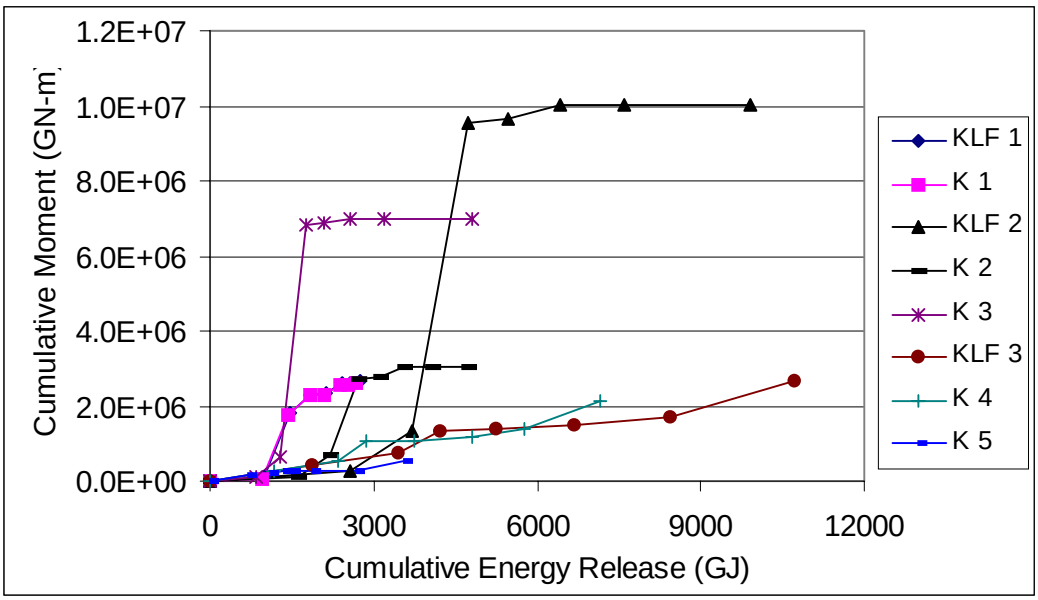

Figure 6.2 Cumulative moment vs. cumulative energy release for the three regions and five sub-regions at Kloof Gold Mine.

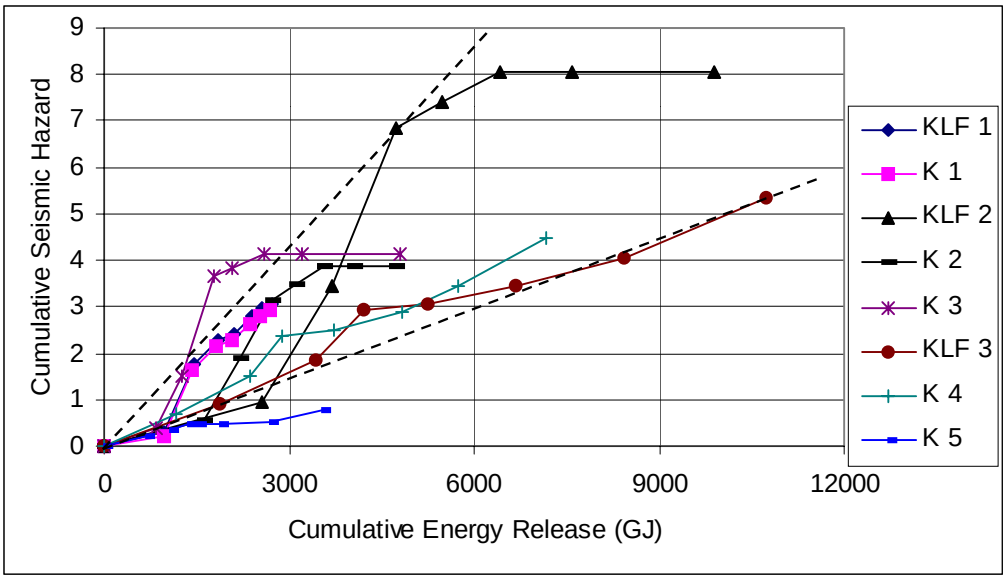

Figure 6.3 Cumulative seismic hazard vs. cumulative energy release for the seismogenic regions and sub-regions at Kloof Gold Mine. The dashed lines indicate two slopes, separated by a factor of three.

As mentioned earlier, the jumps caused by the larger events dominate the ΣM_0 plots in Figures 6.2. In Figure 6.3 we see smoother curves, suggesting that each region and sub-region has a characteristic "efficiency" of converting total elastic energy release into seismicity. This is the single most important observation in this project. Having exhibited a certain rate of seismicity per unit of energy release, each sub-region keeps to this rate.

The different regions and sub-regions show a variation of about a factor of three. The steeper dashed line indicates that some regions are more active than others, **even when normalised to both ERR and area mined**. The need for careful normalisation cannot be stressed too strongly.

The most active sub-regions were K2 and K3. In Figure 6.1 we can see that the mining was both deeper and was adjacent to more extensively mined-out areas. K5 is the least active. It is both shallow and remote from other mined-out areas.

Finally, we show the more conventional plot of seismicity per area mined as a function of ERR for the same data points as used in Figure 6.3 and in Figure 6.4. Although there is

some increase of seismicity with increasing ERR, the correlation is very poor. The range of seismicity would decrease by grouping the data into longer periods of time, but so would the range of ERR. The benefit of using the cumulative plots is immediately clear.

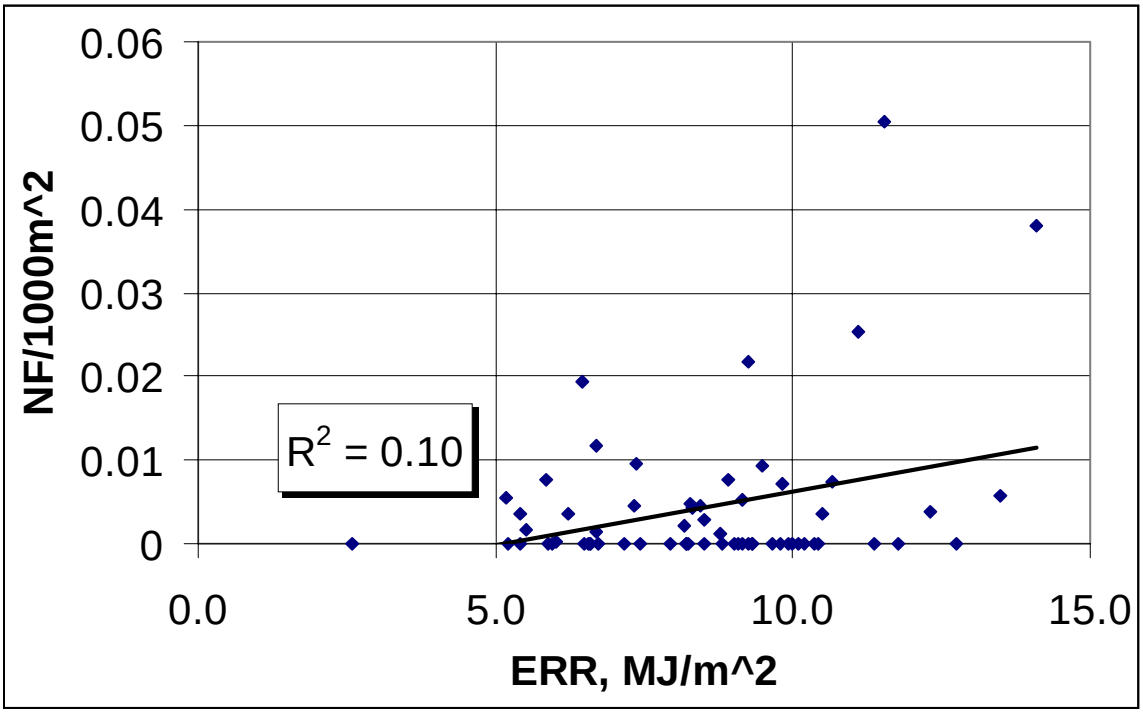

Figure 6.4 Seismicity per area as a function of ERR at Kloof mine.

6.1.2 Elandsrand Gold Mine

Elandsrand Gold Mine contains only one geotechnical area, namely "hard"' (Alberton) lava hangingwall with quartzite-conglomerate footwall. The seismic data set consisting of 70 063 seismic events recorded by the ISS seismic system over the period 1993 to 1995, with magnitudes in the range of -2.0 to 3.8, was analysed.

Generally the seismicity on this mine is characterised by a large number of small seismic events. A plot of seismic locations for events with $M \geq 1.0$ is shown in Figure 6.5. The majority of the seismic events are concentrated in two regions to the West and to the East. A narrow area lying between them is characterised by limited mining and seismicity.

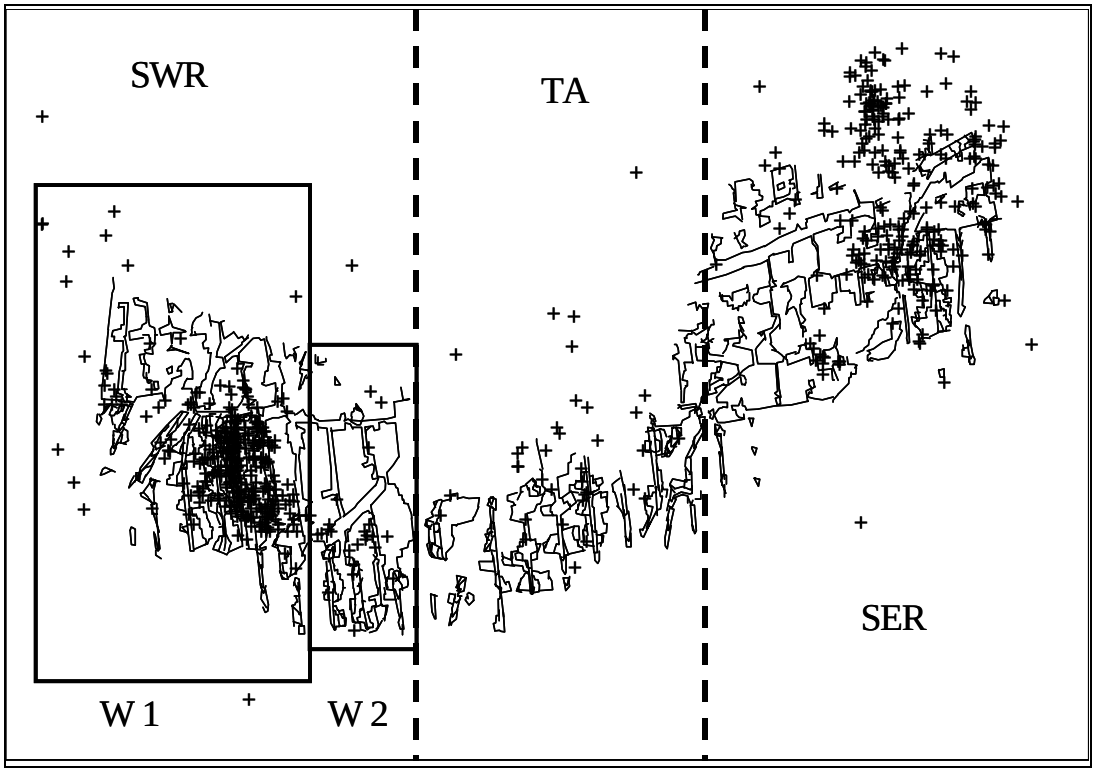

Figure 6.5 Elandsrand Gold Mine: A plot of seismic locations for events with $M \geq 1.0$

Given the size of an entire mine, the MINF modelling was done in three windows, marked SWR, TA and SER. Furthermore, SWR was subdivided into two sub-regions W1and W2. The results are shown in Figures 6.6 and 6.7.

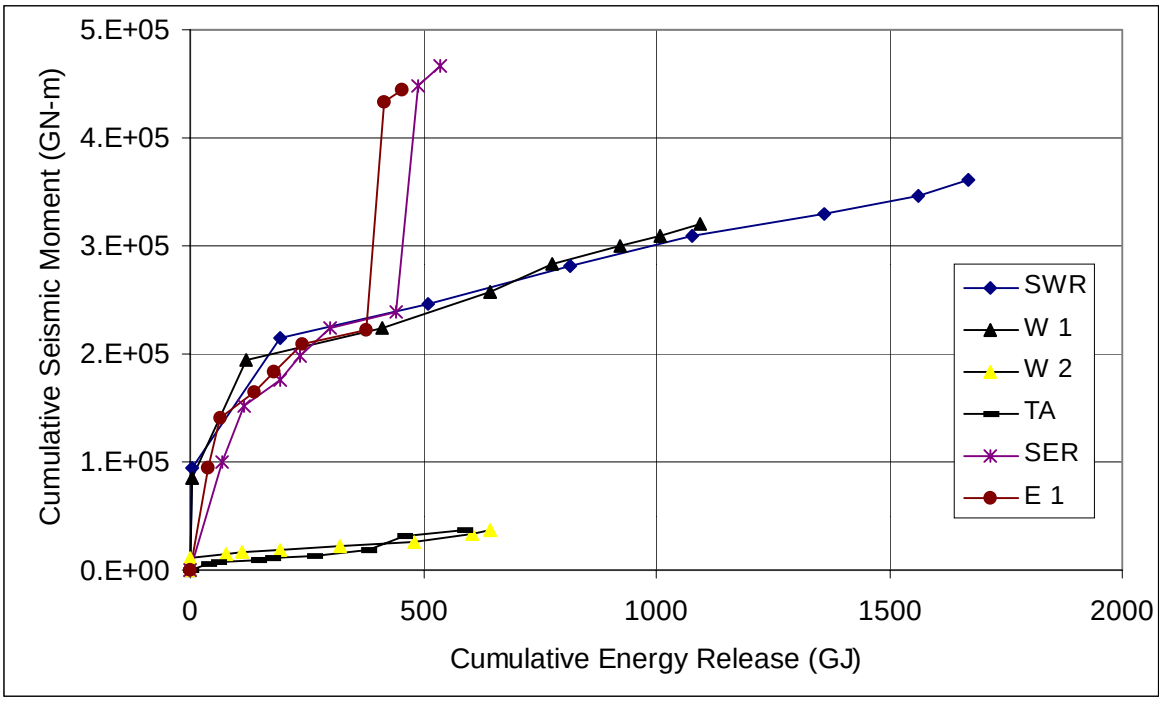

Figure 6.6 Cumulative moment vs. cumulative energy release calculated for three seismogenic regions at Elandsrand Gold Mine

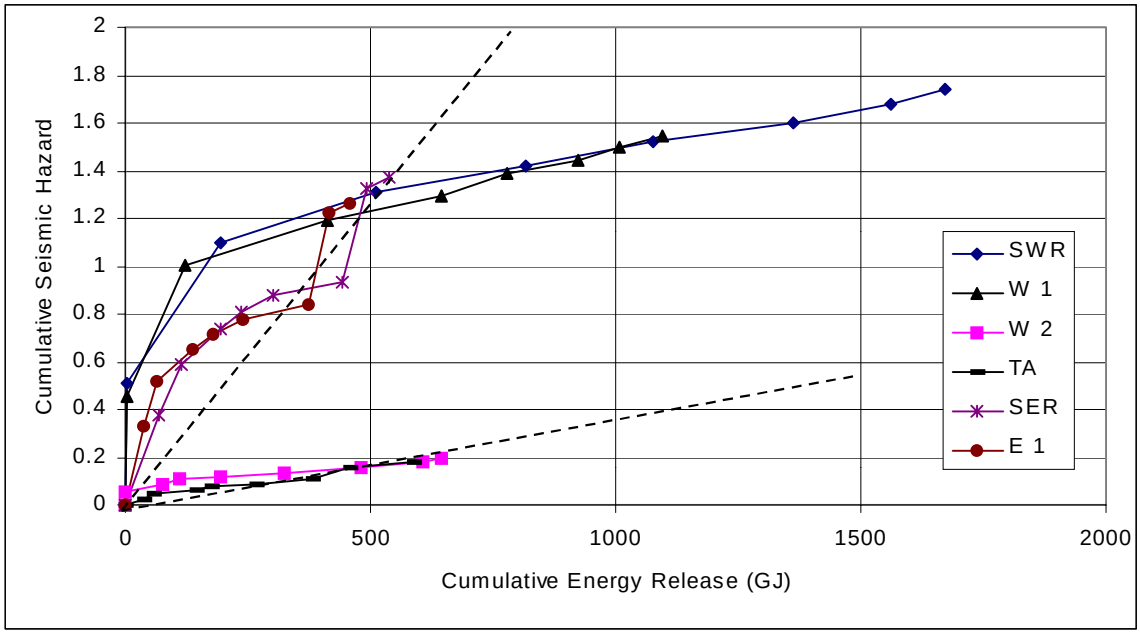

Figure 6.7 Cumulative seismic hazard vs. cumulative energy release calculated for two seismogenic sub-regions from Southwest part of Elandsrand Gold Mine

6.2 Carbon Leader

We used data time periods between June 1996 and September 1998 for data from the WD336 area at Western Deep Levels mine. This data set is being studied in more detail under the Deepmine project 5.2.1. In this case, we only analyse data for one area. As before, it also shows a characteristic rate of seismicity per elastic energy release.

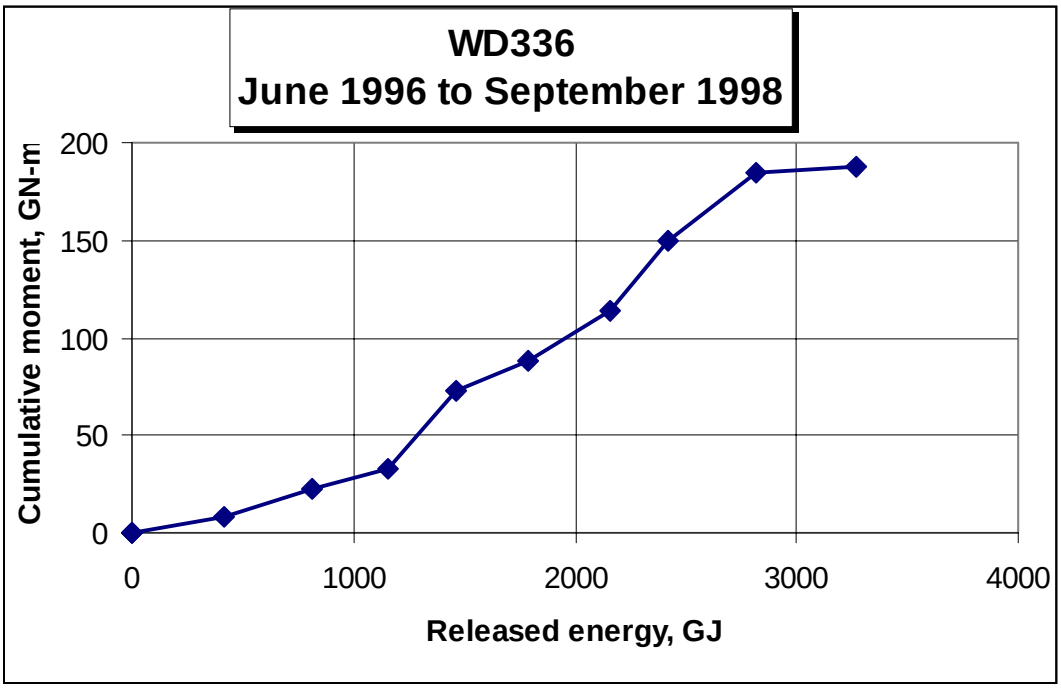

Figure 6.8 Seismic moment as a function of released energy at WD336.

6.3 Vaal Reef

Although this project only asked for an analysis of data from the VCR and Carbon Leader (CLR) reef, we show some recent work done on the Vaal Reef (Andersen et al, 1999). Although the Vaal Reef is typically much more faulted than the VCR or CLR and ERR is not used as a mine design criterion, we see similar patterns in Figures 6.10 and 6.11 that we see for the VCR and CLR. In particular:

- The ΣN_F plots are smoother than the ΣM_o plots.
- Each area is characterised by a linear behaviour in Figure 6.11, implying a constant "efficiency" of converting elastic ERR into seismicity.

- The differences in seismic “efficiency” between different areas in very pronounced. This is probably the result of the greater in influence of faulting of the Vaal Reef.

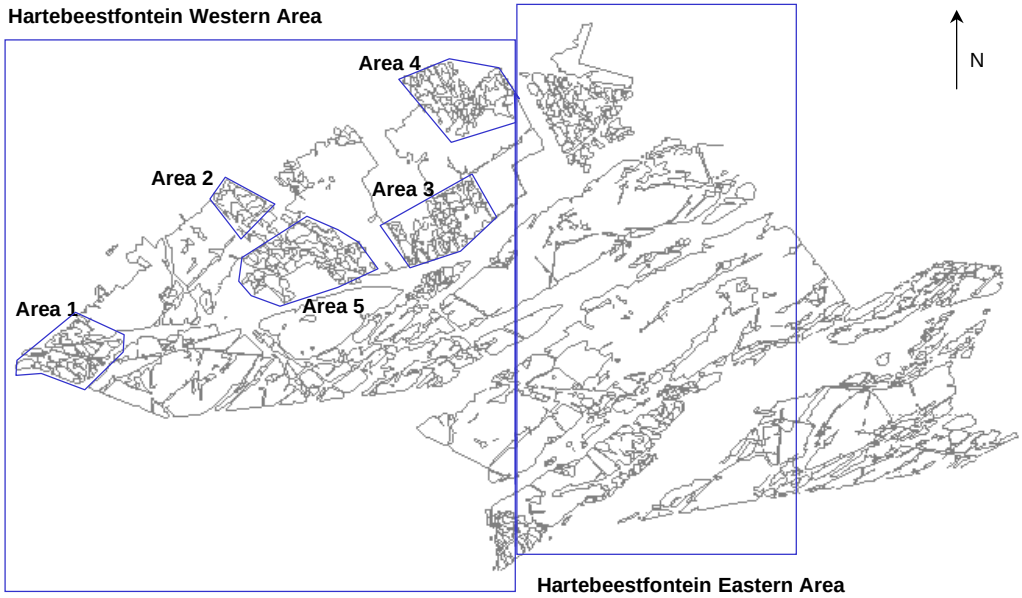

Figure 6.9 Selected areas in Hartebeestfontein mine (From Andersen et al, 1999).

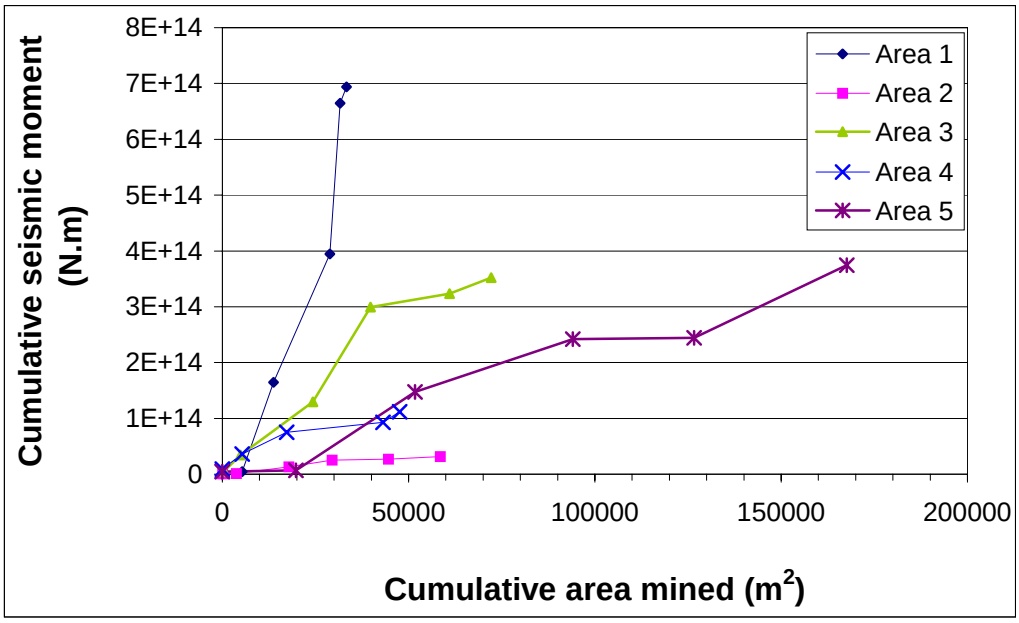

Figure 6.10 Variation of the cumulative seismic moment with area mined for five polygons defined at Hartebeestfontein G.M. (From Andersen et al, 1999).

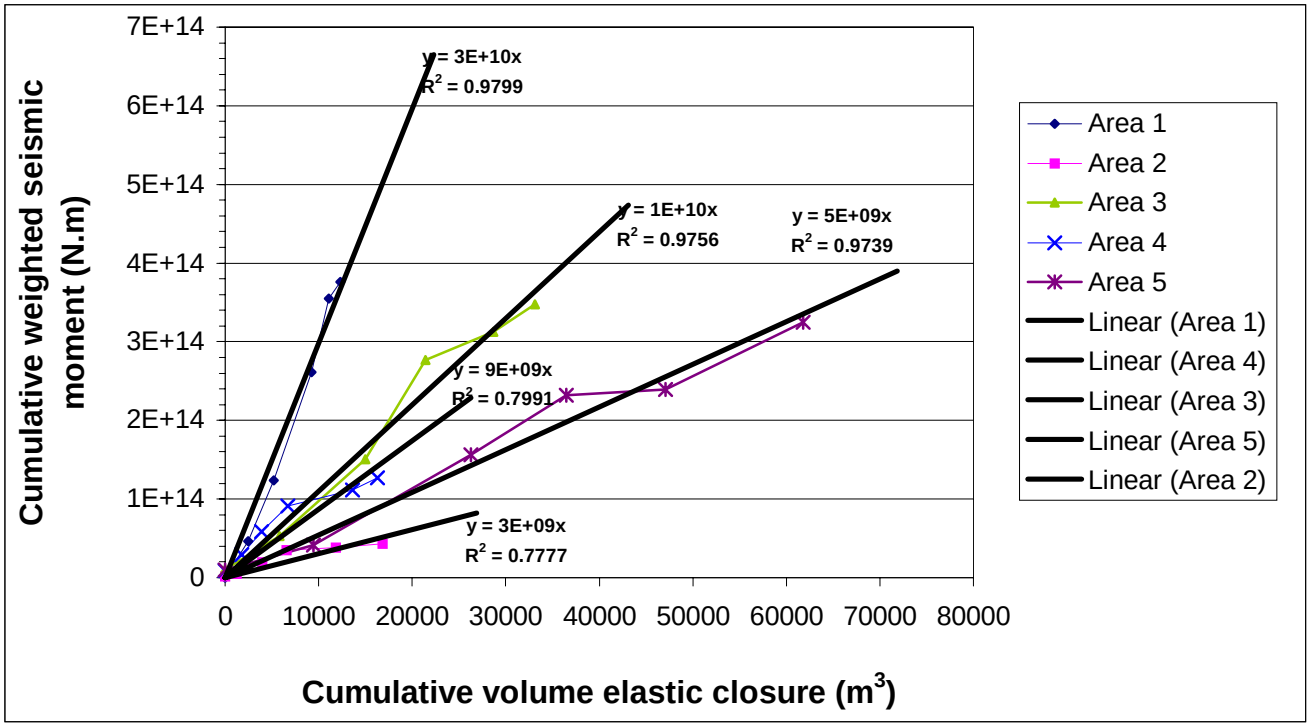

Figure 6.11 Variation of cumulative weighted seismic moment (ΣN_F) with volume of elastic closure for five polygons defined at Hartebeestfontein G.M. Linear fits to the data are extrapolated for 10 000 m^3 of additional elastic closure. (From Andersen et al, 1999).

7 Error analysis

There are numerous possible sources of error in applying ERR as a mine design criterion based on work that relates seismicity to energy release. We now consider sources of error in four categories.

1. The relationship between seismicity and rockbursts is not well understood. We do not know under what conditions a seismic event will cause damage.

2. None of the relationships considered to date have suggested that there is a level of ERR below which seismic events do not occur. We cannot therefore say that, if the ERR were reduced through improved mine layout or the use of backfill, a particular rockburst would not have happened. We can only say that the probability of an event of any size could be changed. The probabilistic nature of

these relationships has profound legal implications. It is also provides no consolation to unlucky victims of rockbursts.

3. In back analyses, such as those performed in this report, the choice of areas and times for quantifying seismicity is always somewhat arbitrary. In Figure 7.1 we show the results of a Monte Carlo simulation of 50% of the events in a typical data set. The effect of including or excluding events at random can be large when ΣM_o is used, but is acceptable when ΣN_F is used.

4. The modelling of ERR is obviously prone to numerous errors too. Much progress has been made on the entire issue of what rock properties to use and how to apply them. As has been indicated, there are still large gaps in our knowledge. Accurate modelling within these bounds seems to hinge on the number of elements used in the model, particularly across pillars. For multi-step mining, the error in energy release is proportional to $1/\sqrt{N}$.

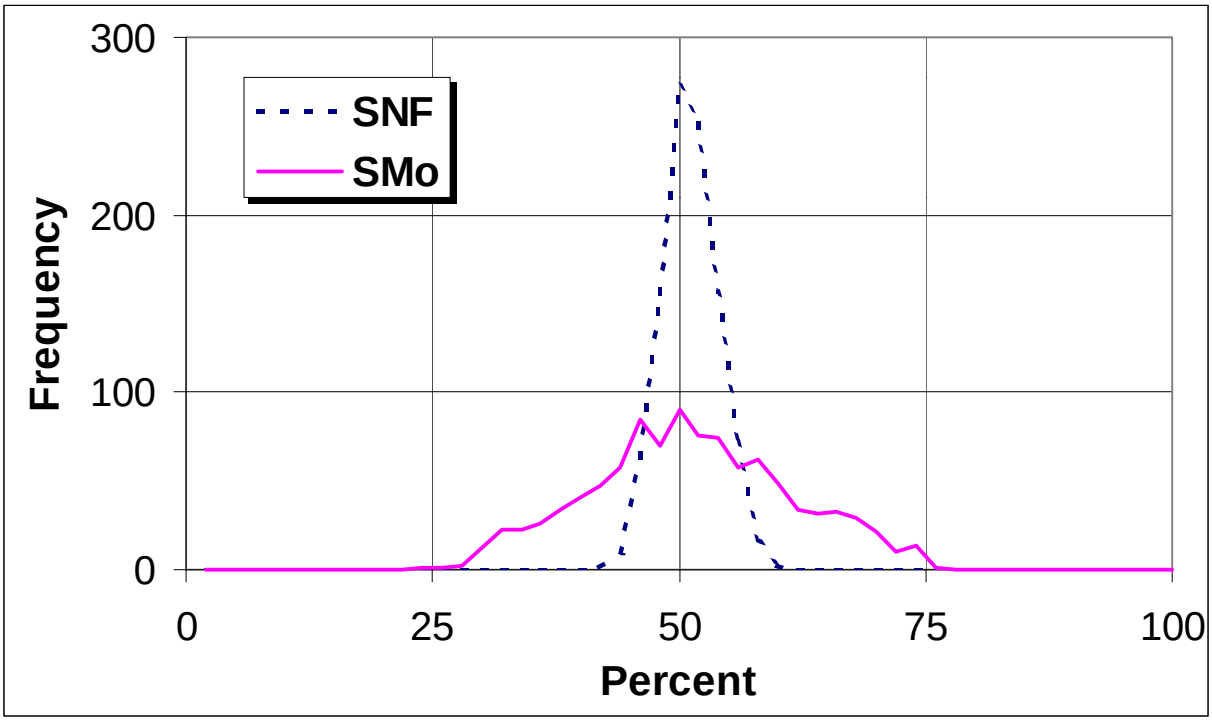

Figure 7.1 Distribution of ΣM_o and ΣN_F from 1000 Monte Carlo simulations of a typical data set.

8 Discussion

The many figures relating seismicity to elastic energy release show more variation in the rate of seismicity between regions and sub-regions than over time within any region. What impact might this have on mine design?

A mine starts mining two areas “A” and “B” and mines at the rate of 25 000 m^2 per annum and at an average ERR of 20 MJ/m^2 in each area. After one year, total elastic energy released in each area was 500 GJ. Due to local variations in virgin stress or some kind of geotechnical behaviour, region “B” was found to be three times as active as region “A”, as listed in Table 4.

The mine now decides to take action to reduce the future seismicity in area B by reducing the ERR from 20 MJ/m^2 to 10 MJ/m^2. As the mine is only committed to maintaining an average of 20 MJ/m^2, it is also decided to allow the average ERR in area B to increase from 20 MJ/m^2 to 30 MJ/m^2. This does not increase the average ERR for the mine.

	Year1	Year 2
Area A, 10^3 m^2	25	25
Area B, 10^3 m^2	25	25
ERR A, MJ/m^2	20	30
ERR B, MJ/m^2	20	10
Seismicity, A	10	15
Seismicity, B	30	15
Seismicity, A+B	**40**	**30**

Table 4

If the rate of seismicity per energy released remains constant in each area, then area B will experience a 50% decrease in the number of seismic events and area A will see a 50% increase in seismicity. The net result, in this hypothetical model, is that 25% fewer events should occur in the two areas year 2 compared to year 1.

9 Conclusions

Since the early 1960's, reduction of the volume of elastic convergence through the use of regional stability pillars has been the principal means of controlling mining-induced seismicity. This control measure has been exercised through limiting the average Energy Release Rate (ERR) to some figure, typically 20 or 30 MJ/m^2. Mines have responded by leaving large areas of reef as regional stability pillars. It has been found that seismicity has indeed decreased, but damaging seismicity has still occurred on active faces and even on the stability pillars. A re-assessment of ERR has therefore been needed.

We report here on a re-analysis of previous work on the relationship between ERR and seismicity. Data from four mines spanning the Ventersdorp Contact, Carbon Leader and Vaal Reefs were analysed using the MINF suite of programs. Results were not in contradiction with previous work, but help to refine and consolidate certain ideas.

Based on our analysis, we recommend the following for application of ERR to current mine layout design:

1. The choice of value of ERR to be used must be made at each mine on the basis of local experience with rockburst damage.

2. The mine's average ERR should be calculated from values at all the working places.

3. Localised high values of ERR should not be excluded when averages are calculated. Under these conditions, there might not be an equivalently high rate of seismicity and rockbursting. This energy has already been released by earlier mining. These high values of ERR should therefore still be considered as contributing to the overall potential for seismicity.

4. When high values of ERR are encountered, the area should be mined using special, or remnant, precautions.

5. There are large variations in the amount of seismicity per elastic energy release in different areas. This variation exceeds the effect that changes in modulus or stoping width would have on ERR. Within any single area, the rate of seismicity per energy release is almost constant, varying by less than the variations between areas.

6. A mine may wish to reduce ERR in areas of higher seismicity per energy release and increase ERR is areas of lower seismicity per energy release, as long as the nominated average ERR is not increased. ERR could be **decreased** by various means, such installing backfill, decreasing spans or increasing pillar sizes. In the extreme, faces could be stopped. ERR could be **increased** by, for example increasing spans or decreasing pillar sizes.

7. Mines should continue using their current values of moduli and stope width. In general, a Young's modulus of about 70 GPa is used at mines. Lower values have been suggested to account for the greater amount of closure and stresses on backfill. Adjusting these parameters will not make up for the variations between areas noted in point 4.

8. Calculation of ERR through multi-step mining is numerically very consistent and is independent of grid size and order of mining. This method is consistent with the concept of the volume of elastic convergence. We recommend that computer programs that report ERR use this method when ERR is used as an indicator of seismicity.

9. We recommend that mines establish the practice of routine digitising and modelling, or continue it where it is being done. Quantitative comparison with seismicity should be done routinely to identify those areas with an anomalously high or low rate of seismicity.

Further research in this area will most likely improve correlations between observed and modelled seismicity. This will be the main thrust of the GAP722 project starting in April 2000. The final objective of this project will be to provide more accurate tools for mine design. In doing this, we expect to obtain further insights into what controls the amount and character of seismicity.

10 Acknowledgements

Gratitude is expressed to SIMRAC for financial support of project GAP 612c. Discussions with Dr. John Ryder have contributed towards some of the ideas explored in the paper. Thanks to Francois Malan and Ewan Sellers for providing digital copies of figures. The contribution of Figures 6.9 to 6.11 from the Deepmine project 5.2.1 is gratefully acknowledged.

11 References

Andersen, L., Spottiswoode, S. and Sellers E. 1999 Investigation of new and revised criteria for the integration of seismic monitoring and numerical modelling, Unpublished report, Deepmine project 5.2.1.

Anon. 1988. An industry guide to methods of ameliorating the hazards of rockfalls and rockbursts. Chamber of Mines research Organisation. 1988 edition

Bosman, J.D. 1999. Bracket pillar design – a case study. Proc. 2nd Southern African Rock Engineering Symposium, Ed. TO Hagan, ISRM Regional Symposium, pp15-20.

Cook, N.G.W, Hoek, E., Pretorius, J.P.G, Ortlepp, W.D. and Salamon, M.D.G. 1966. Rock Mechanics applied to rockbursts. J. S. Afr. Inst. Min. Metall. : 435-714.

Dunn, M.J. and Laas, J.J. 1999. Design of the African Rainbow Minerals No.5 Shaft pillar extraction. Proc. 2nd Southern African Rock Engineering Symposium, Ed. TO Hagan, ISRM Regional Symposium, pp21-27

Gürtunca, R.G. and Adams, D.J. 1991. Determination of the in situ modulus of the rockmass by the use of backfill measurements. J.S. Afr. Inst. Min. Metall. 91, pp81-88.

Heunis, R., 1980. The development of rockburst control strategies for South African gol mines. J.S. Afr. Inst. Min. Metall., vol80.

Hildyard, M.W. and Milev, A. 1999 Modelling seismic wave interaction with a tunnel due to an artificial rockburst. Proc. 2nd Southern African Rock Engineering Symposium, Ed. TO Hagan, ISRM Regional Symposium, pp273-280.

Johnson, J.C., Larson, M.K., Brady, T.M., Whyatt, J.K., Langston, R.B. and Kirsten, H. 1999 Stress measurements of a jointed rock mass during drift development. Proc. 2nd Southern African Rock Engineering Symposium, Ed. TO Hagan, ISRM Regional Symposium, pp94-102.

Jordon, T.J. 2000. Unpublished presentation at ISS seminar, March 7th, Stellenbosch.

Kuijpers, J.S. 1999. Fracturing around over-stressed circular openings in brittle rock. Proc. 2nd Southern African Rock Engineering Symposium, Ed. TO Hagan, ISRM Regional Symposium, pp108-114.

Lachenicht, R.J. and van Aswegen, G. 1999. An engineering method to evaluate the seismic potential of geological structures as a function of mine layout. Proc. 2nd Southern African Rock Engineering Symposium, Ed. TO Hagan, ISRM Regional Symposium, pp233-237.

Malan, D.F. 1999. Time dependent behaviour of deep level tabular excavations in hard rock. Rock Mech. Rock Eng. 32 (2), 123-155.

McGarr, A. 1976. Seismic moment and volume changes, J. Geophys. Res.,81, 1487 - 1494.

McGarr, A., Spottiswoode S.M and Gay N.C. 1975. Relationship of mines tremors to induced stress and to rock properties in the focal region. Bull. Seism. Soc. Am., 65 : 981-993.

McGarr, A. and Wiebols, G.A. 1977. Influence on Mine Geometry and closure volume on Seismicity in deep level mine. Int. J. Rock Mech. Min. Sci., & Geomech. Abstr., 14:139-145.

Milev, A. and Spottiswoode, S.M. 1997. Integrated seismicity around deep-level stopes in South Africa. Int. J. Rock Mech. & Min. Sci. Vol. 34:3-4, Paper No. 199.

Napier, J.A.L. and Stephansen, S.J. 1987. Analysis of deep-level mine design problems using MINSIM-D boundary element program. APCOM 87, SAIMM, Johannesburg : 3-19.

Napier, J.A.L. 1991. Energy changes in a rock mass containing multiple discontinuities. J. S. Afr. Inst. Min. Metall. 91 : 145-157.

Napier, J.A.L. and Peirce, A.P. 1995. Simulation of extensive fracture formation and interaction in brittle materials. Mechanics of jointed and faulted rock – 2, Rossmanith (ed), Balkema: Rotterdam pp 63-75.

Napier, J.A.L and Malan, D.F. 1997. A viscoplastic discontinuum model of time-dependent fracture and seismicity effects in brittle rock. Int.J. Rock mech. Min. Sci., 34 : 1075-1089.

Oelofse, J.M. and Judeel, G.du T. 1999. Tunnelling through the Running Dyke on Tau Lekoa Mine – Vaal River Operations. Proc. 2nd Southern African Rock Engineering Symposium, Ed. TO Hagan, ISRM Regional Symposium, pp101-107.

Ozbay, M.U., Spottiswoode, S.M. & Ryder, J.A. 1993. A quantitative analysis of pillar-associated large seismic events in deep mines. 3rd Intl Symposium on Rockbursts and Seismicity in mines, Balkema :107-110.

Rangasamy, T., Jiyana, L. and Pethö, S.Z. 1999. Support design, implementation and monitoring in the South Deep shaft system, Placer Dome Western Areas Joint Venture. Proc. 2nd Southern African Rock Engineering Symposium, Ed. TO Hagan, ISRM Regional Symposium, pp218-227.

Peirce, A.P. Spottiswoode S.M. and Napier J.A.L. 1992. The spectral boundary element method : a new window on boundary elements in Rock Mechanics. Int J Rock Mech Min Sci & Geomech Abstr, 29 (4) : 379-400.

Roberts, D.P., Sellers, E.J. and Sevume, C. 1999. Numerical modelling of fracture zone development and support interaction for a deep-level tunnel in a stratified rockmass. Proc. 2nd Southern African Rock Engineering Symposium, Ed. TO Hagan, ISRM Regional Symposium, pp264-272.

Roberts, M.K.C., Eve, R.E., Jager, A.J., Schweitzer J.K., Guler, G., Quaye, G., Milev, A.M., Glisson, J., Kuijpers, J.S. 1997. Improved support design by an increased understanding of the rock mass behaviour around the Ventersdorp Contact reef, Safety in mines research advisory committee (SIMRAC), Final Project Report GAP 102. Pretoria: Department of Minerals and Energy

Ryder, J.A. and Napier, J.A.L. 1985. error analysis and design of a large scale tabular mining stress analyser. Int. Conf. Num. Meth. in Geomech. Nagoya (Japan). pp 1549-1555.

Salamon, M.D.G. 1984. Energy considerations in rock mechanics: fundamental results. J.S. Afr. Inst. Min. Metall., 84, 233-246.

Sellers, E.J. 1997. A tessellation approach for the simulation of the fractures zone around a stope. . Proc. 1st Southern African Rock Engineering Symposium, Ed. RG Gürtunca and TO Hagan, SANGORM, 143-154.

Simon, R., Mitri, H.S and Aubertin M. 1999. A comparative study of non-linear constitutive models for rock joints. Proc. 2nd Southern African Rock Engineering Symposium, Ed. TO Hagan, ISRM Regional Symposium, pp 281-286.

SIMRAC 1999. Numerical modelling of mine workings, GAP415.

Singh, N. and MacDonald A.J. 1999. Extraction of a wide orebody at depth in the SV2/3 area at Placer Dome Western Areas Joint Venture. Proc. 2nd Southern African Rock Engineering Symposium, Ed. TO Hagan, ISRM Regional Symposium, pp 351-359.

Spencer, D. and York, G. 1999. Back analysis of yielding pillar behaviour at Impala Platinum Mine. Proc. 2nd Southern African Rock Engineering Symposium, Ed. TO Hagan, ISRM Regional Symposium, pp44-52.

Spencer, D. 1999. A case study of a pillar system failure at shallow depth in a chrome mine. Proc. 2nd Southern African Rock Engineering Symposium, Ed. TO Hagan, ISRM Regional Symposium, pp53-59.

Spottiswoode S.M. 1988. Total seismicity, and the application of ESS analysis to mine layouts. J. S. Afr. Inst. Min. Metall. (88) : 109-116.

Spottiswoode S.M. 1990. Towards 3-dimensional modeling of rock deformation around deep-level gold mines. Mechanics of Jointed and Faulted Rock, Rossmanith (ed.), Balkema, Rotterdam: 1133-1146.

Spottiswoode S.M. 1997. Energy Release rate with limits to on-reef stress. Proc. 1st Southern African Rock Engineering Symposium, Ed. RG Gürtunca and TO Hagan, SANGORM, 252-258.

Spottiswoode S.M. 1999. Modelling seismicity and creep on multiple stope-parallel layers Proc. 2nd Southern African Rock Engineering Symposium, Ed. TO Hagan, ISRM Regional Symposium, pp155-159.

Stacey, T.R. and Wesseloo, J. 1999. Extension strain fields ahead of the “face” of a tunnel or shaft and potential effects on excavation performance. Proc. 2nd Southern African Rock Engineering Symposium, Ed. TO Hagan, ISRM Regional Symposium, pp125-131.

Tang, B., Mitri, H.S., Marwan, J. and Comeau, W. 1999. 3-dimensional modelling of distress blasting. Proc. 2nd Southern African Rock Engineering Symposium, Ed. TO Hagan, ISRM Regional Symposium, pp 287-292.

van Antwerpen , H.E.F and Spengler, M.G. 1982. The effect of mining-related seismicity on excavations at East Rand Proprietary Mines, Limited, Proceedings of the First International Symposium on Rockbursts and Seismicity in Mines, Johannesburg, S. Afr. Inst. of Min. Metall : 235-244.

Vieira FMCC, 1997. Review of criteria for stabilising pillars, Proc. 1st Southern African Rock Engineering Symposium, Ed. RG Gürtunca and TO Hagan, SANGORM, 210-227.

Vieira, F.M.C.C. 1999. The evaluation of the rock engineering aspects of SMDP mining at great depth an dthe use of a multiple-attribute utility for mine layout assessment. Proc. 2nd Southern African Rock Engineering Symposium, Ed. TO Hagan, ISRM Regional Symposium, pp 310-323.

Watson, B.P. and Roberts, D. 1999. A new approach to designing safe panel spans on the Merensky Reef. Proc. 2nd Southern African Rock Engineering Symposium, Ed. TO Hagan, ISRM Regional Symposium, pp 324-330.

York, G, Cambulat, I., Kebaya, K.K., le Bron, K.B. and Williams, S.B. 1999. In panel pillar system design in shallow to intermediate depth hard rock mines. Proc. 2nd Southern African Rock Engineering Symposium, Ed. TO Hagan, ISRM Regional Symposium, pp60-68.